Morphology and Micromechanical Deformation Behavior of Styrene/Butadiene-Block Copolymers. I. Toughening Mechanisms in Asymmetric Star Block Copolymers

G. H. MICHLER,[1] R. ADHIKARI,[1] W. LEBEK,[1] S. GOERLITZ,[1] R. WEIDISCH,[2] K. KNOLL[3]

[1] Institute of Materials Science, Martin-Luther University Halle-Wittenberg, 06099 Halle, Germany

[2] Polymer Science and Engineering Department, University of Massachusetts, Amherst, Massachusetts 01003

[3] BASF Aktiengesellschaft, Polymers Laboratory ZKT/I-B1, D-67056 Ludwigshafen, Germany

ABSTRACT: Lamellae-forming styrene/butadiene star block copolymers are studied to investigate the influence of morphology on micromechanical deformation mechanisms and mechanical properties by using transmission electron microscopy and tensile testing. A large homogeneous plastic deformation of polystyrene (PS) lamellae is found in styrene/butadiene star block copolymers on the basis of the new mechanism called thin-layer yielding. This mechanism depends strongly on the thickness of the PS lamellae. At a critical thickness of PS lamellae of about 20 nm, a transition from thin-layer yielding mechanism to a crazelike deformation was observed. These new deformation zones are similar to crazes with respect to their propagation perpendicular to direction of external stress and similar to shear bands with respect to an internal shear deformation component of the lamellae in the deformation zones. As a result of our investigations, the mechanical properties of star block copolymers can be understood in correlation with morphology and micromechanical deformation mechanisms. © 2002 Wiley Periodicals, Inc. J Appl Polym Sci 85: 683–700, 2002

Key words: SB star block copolymers; thin-layer yielding; toughening mechanism; morphology; micromechanical mechanisms; electron microscopy

INTRODUCTION

For many applications of polymers, toughness is an important property. It has been well known for many years that the fracture toughness can be increased up to one order of magnitude by an incorporation of a small amount of elastomer in thermoplastics. This effect was initially utilized in polystyrene (PS) and styrene-acrylonitrile (SAN) copolymers by grafting to butadiene rubber to yield high-impact polystyrene (HIPS) and acrylonitrile-butadiene-styrene copolymer (ABS), respectively. Meanwhile, many other thermoplastics were modified with various elastomers.

In high-impact polymer systems with disperse structure, the thermoplastic component forms the matrix in which the rubber phase is dispersed as particles. In these disperse systems, there are two categories of toughening mechanisms: either the energy absorbing step is the preferred formation

of crazes at the rubber particles (multiple crazing), as in HIPS or numerous ABS grades; or the energy absorption mainly takes place through shear deformation between the modifier particles (multiple shearing) as in impact-modified polyamide (PA) or polypropylene (PP).[1,2]

A general disadvantage of these modifications is a pronounced decrease of strength and stiffness of the toughened polymers. However, a good balance of these properties in combination with other properties and a good processability is demanded for many usual applications of polymers. Recently, some new micromechanical mechanisms were found as alternative mechanism to the classical toughening mechanism of multiple crazing or multiple shearing, such as the core-yielding mechanism in SAN modified with core-shell particles.[3]

In recent years, discovery of new fascinating morphologies in ABC triblock copolymers, star block copolymers, and block copolymer/homopolymer blends have opened up new possibilities of controlling morphology and thereby mechanical properties of the block copolymers.[4–10] A wide variety of interesting microphase-separated structures were reported in three-component block copolymers and their blends.[9,10] Advancement in different synthetic routes have enabled the preparation of block copolymers beyond the imagination of chemists. Theoretical works have predicted even more new morphologies in such systems that are yet to be discovered.[11,12]

Block copolymers generally show different deformation mechanisms compared to those of homopolymers because of the microphase-separated morphologies (e.g., structures in the nanometer scale are often too small to initiate crazes).[5,13,14] Therefore, deformation mechanism in diblock copolymers is much different from the crazing mechanism in PS. Schwier et al.[14] proposed a model for craze growth in polystyrene-*b*-polybutadiene diblock copolymers on the basis of a mechanism of cavitation in the PB domains under the concentrated stresses of the craze tip. In PS, local stress fields initiate the formation of crazes consisting of thin-craze fibrils. The undeformed PS material will be transformed into craze fibril material (highly deformed PS) via a surface-drawing mechanism. In contrast to crazing in PS, in block copolymers the first step of deformation is always the deformation of the rubber phase up to a critical stress.[4,14] This is followed by the formation of voids. The second step is the deformation of the glassy matrix under elevated stresses between the cavities. The growth of crazes occurs by different mechanisms in PS (surface drawing mechanism) and in diblock copolymers (cavitation and deformation of matrix strands).

Star block copolymers are earning special attention because of their superiority in mechanical properties over their linear analogues.[15–17] The asymmetric star block copolymers are particularly interesting in this respect. A great deal of investigation was carried out theoretically as well as experimentally regarding phase behavior and mechanical properties of star block copolymers. Star block copolymers have been found to possess lower melt viscosity, which manifests their better processability than triblock copolymers with similar molecular weight.[15–17] Of special technical importance are the tapered block copolymers.[18–21] Limited work has been done, however, regarding the correlation between microstructures, mechanical properties, and micromechanical deformation behavior of these types of block copolymers.

An interesting material in this respect is the asymmetric styrene-butadiene star block copolymer produced by BASF known as Styrolux®.[21] In the present study, several samples of this material are investigated to understand mechanical properties based on micromechanical mechanisms of deformation and fracture. Mechanical properties and morphology are qualitatively as well as quantitatively characterized by means of uniaxial tensile tests and transmission electron microscopy (TEM), respectively. In subsequent articles, blends of these star block copolymers with PS and other copolymers with different constitutions will be described.

EXPERIMENTAL

Materials and Sample Preparation

The characteristic data of the samples used in this study are shown in Table I. For a better understanding of micromechanical processes and mechanical properties in relation to structure formation and morphology developments, solution cast films as well as injection-molded samples were investigated. Synthesis of the block copolymers used in the present study was discussed by Knoll and Nieβner.[21] The star block copolymers used in this study have about four arms. In addition, all samples are asymmetric with respect to the length of the PS arms (e.g., one of the PS arms

Table I   Molecular Weight and Composition of Asymmetric Styrene-Butadiene Star Block Copolymers Used in This Study

Group	Materials	M_n	M_w/M_n	Φ_{PS}	Φ_{GPPS}[a]
I	sample I	118,900	1.91	74	17
II	Sample IIa	100,400	1.96	74	14
	Sample IIb	109,200	1.69	74	0
III	Sample III	95,200	1.91	80	17
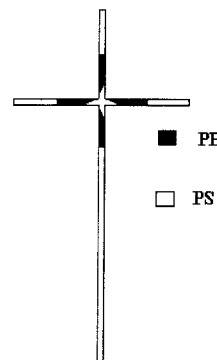
Note. The molecular structure of the star block copolymer ST2-S74 is schematically illustrated in the diagram on the right side. All the star block copolymers have analogous molecular structures.

[a] Weight fraction of added GPPS general purpose polystyrene.

has a higher molecular weight). All star block copolymers used in the present study consist of a PS core with a tapered transition to PB. The molecular characteristics are given in Table I.

Few samples contain general purpose polystyrene (GPPS) prepared by radical polymerization, which has a number-average molecular weight of 190,000 g/mol and polydispersity index of 2.3.

Sample Preparation

Samples used for the present study are categorized in three groups. The basic star block copolymer used is named as ST2.

I. Samples with lamellar structure and GPPS particles (ST2-S74 containing 17 wt % of general purpose polystyrene, GPPS, solution cast films);

IIa. Samples with lamellar structure without GPPS particles. These samples show neck formation (shrinkage) during tensile tests (ST2-S4 containing 14 wt % of GPPS, injection molded);

IIb. Samples with lamellar structure without GPPS particles (ST2-S74, injection molded and also solution cast films);

III. Samples with lamellar structure without GPPS particles and without shrinkage during deformation (ST2-S80 with reduced PB content, containing 17 wt % of GPPS, injection molded).

Samples containing GPPS particles (sample I) were dissolved in toluene. The solvent was evaporated slowly over 5–7 days at room temperature to get highly ordered equilibrium morphologies. Afterward, the films were annealed to a constant weight in a vacuum oven at 120°C for 3 days. The film thickness was about 0.5 mm. Tensile specimens prepared from these films had a total length of 50 mm.

Samples without GPPS particles (samples IIa, IIb, and III) were prepared by injection molding. Injection-molded samples were processed at a mass and mold temperature of 220°C and 45°C, respectively.

In each paragraph, the detailed description of morphology is followed by an explanation of observed mechanical properties on the basis of micromechanical deformation mechanisms.

Investigations

Mechanical Properties

Tensile tests were performed by using a universal testing machine (Zwick 1425, Ulm, Germany and Instron 4507, Highwycombe, UK) at a crosshead speed of 50 mm/min according to the standards of ISO 3167 and ISO 527. At least 10 samples were measured to prevent preparation effects and to get good statistics of data.

Some of the star block copolymers were tested by varying the crosshead speed (deformation rates: 15–500 mm/min) and temperatures (room temperature, 0°C, −30°C).

Morphology

A small block of each sample cut from the bulk specimen was dipped in aq. OsO_4 solution for several days at room temperature to stain the butadiene phase. Then ultrathin sections ($\sim$ 70 nm) of the samples were cut by using an ultramicrotome (Reichert Ultracut E, Leica, Vienna, Austria) and investigated in a 200-kV TEM (JEOL 2010, Tokyo, Japan). A special image processing program and Fourier transform analysis (FTA) of TEM images were utilized to quantify morphological details.

Micromechanical Mechanisms

After uniaxial tensile tests, a small piece of each sample was cut close to the fracture surface, stained with OsO_4, ultramicrotomed, and investigated by TEM. Changes in morphological details were determined quantitatively by image processing and FTA of the TEM micrographs.

RESULTS AND DISCUSSION

Samples with Lamellar Structure Containing GPPS Particles (Sample I: ST2-S74 containing 17 wt % of GPPS, solution cast films)

Morphology

The typical morphology of this sample (ST2-S74 containing and 17 wt % of GPPS) is the lamellar arrangement of alternating PS and PB lamellae, as shown in Figure 1. This sample was prepared by solution casting by using toluene as solvent.

Because the samples were stained with osmium tetroxide which is absorbed by the PB phase, the PS and PB phases appear white and dark, respectively, in the TEM images. The thickness and long period of PS lamellae are in the range of 12–20 nm and 30–40 nm, respectively. The PB lamellae contain a row of small PS domains (not stained with osmium tetroxide), which look similar to cylinders or spheres having a diameter of 5–9 nm. This observation is consistent with the previous results of Knoll and Nieβner.[21] The lamellae are often bent and curved near GPPS particles. The diameter of the PS particles is between 0.5 and 1 μm.

As already mentioned, sample I is a mixture of the star block copolymer and GPPS. The weight-average molecular weight (M_w) of added GPPS is 190,000 g/mol (polydispersity index, M_w/M_n = 2.3), whereas the longest PS arm of sample I is in the range of 70,000–90,000 g/mol. Studies of block copolymer/homopolymer blends have shown that the molecular weight of the added homopolymer relative to that of corresponding block of the block copolymer is an important parameter with regard to the phase behavior of such blends.[8,22–24] It was shown that in blends of block copolymers and homopolymers, a competition of microphase and macrophase separation occurs if the molecular weight of added homopolymer exceeds that of the corresponding block of the copolymer[8,24] (i.e., at $M_{GPPS} \geq M_{PS\text{-block}}$ the onset of macrophase separation may be found).

In the present case, it is obvious that $M_{GPPS} > M_{PS\text{-block}}$ and a macrophase separation between the added polystyrene (GPPS) and the block copolymer occurs. Because GPPS has a large molecular weight distribution (polydispersity index = 2.3), a part of low molecular fraction of the added GPPS might be dissolved in the corresponding block of the star block copolymer.

Micromechanical Deformation Mechanism

Figure 2 shows details of deformation structure observed in sample I possessing GPPS particles in the Styrolux matrix. Especially, morphological changes around the GPPS particles during deformation are very helpful to understand the micromechanical process.

It is obvious in Figure 2 that the orientation of the lamellae relative to the external stress direction has an important influence on their deformation behavior. A decisive role is played by the GPPS particles which induce a large plastic deformation in the surrounding lamellar matrix.

Growth of microvoids at the poles (i.e., in the direction of stress) of the particles is well known from particle-filled polymers.[2,25,26] In the present case, the GPPS inclusions act as stiff particles embedded in the relatively soft matrix of the star block copolymer. At the pole regions of the stiffer GPPS particles, microvoids appear due to stress concentrations.

If the elastic modulus of the inclusions is much larger than that of continuous matrix, the stress is reduced at the equator of the particles and a compressive stress component at the equators of the spherical GPPS particles yielding a good contact between the particles and the matrix. The maximum stress concentration exists at the poles of the spheres, which is the reason for void formation shown in Figure 2. The PB lamellae can
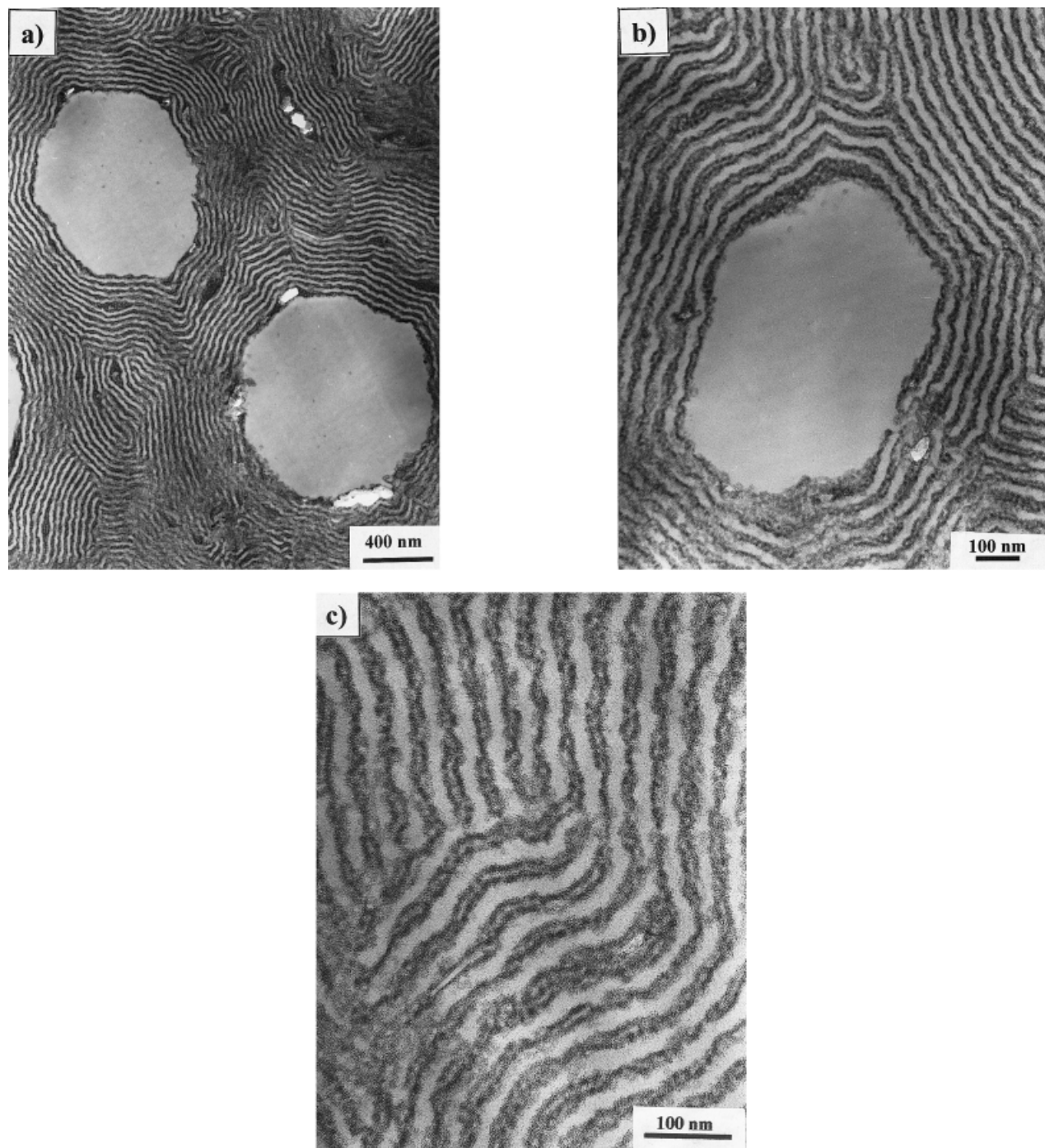
Figure 1   TEM micrographs in different magnifications showing lamellar morphology of sample I (ST2-S74 with GPPS particles; solution-cast film).

cavitate because of their lower cavitation stress (compared to PS lamellae) followed by the formation of voids.[14] However, the cavitation of PB lamellae should occur at a higher stress compared to PS-*b*-PB diblock copolymers because of the presence of additional PS domains inside the PB lamellae.

Formation of microvoids is followed by a large homogeneous plastic deformation of PS as well as the PB lamellae. The contour length of lamellae around a microvoid is about twice of original length at PS particle surface, indicating a local deformation with an extension ratio of about $\lambda = 2$ (i.e., strain, $\epsilon = 100\%$). Lamellae along and
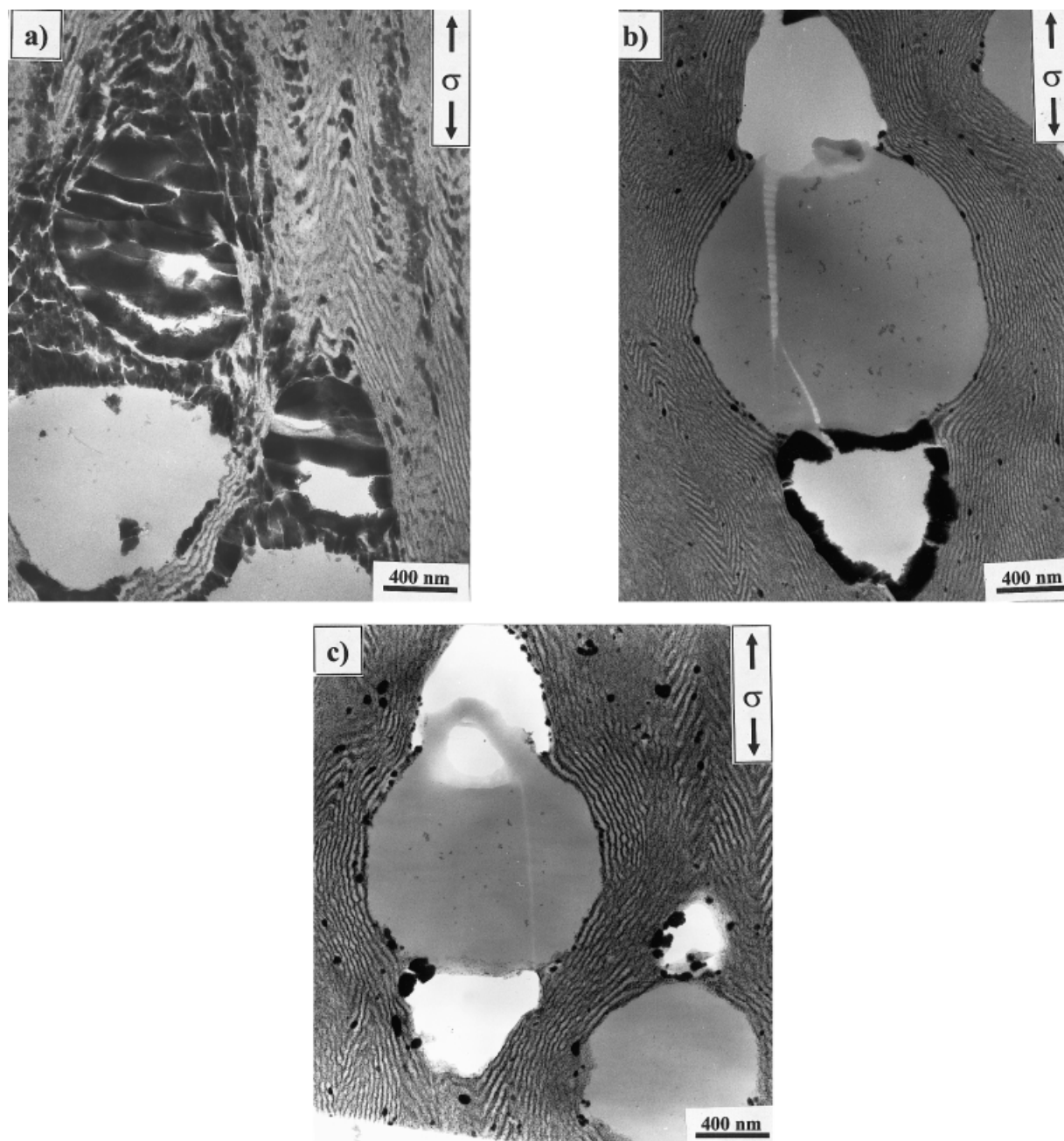
Figure 2 Morphological changes arising from tensile deformation in sample I (ST2-S74 with GPPS particles) with formation of microvoids at the poles of GPPS particles (a–c); crazes in the GPPS particles (a) and deformed and stained PB lamellae oriented perpendicular to the external stress (b); strain direction is indicated by arrows.

between the GPPS particles are also plastically deformed, which results in a transverse stress component in the sample. This transverse stress which is acting back to the GPPS particles is responsible for the initiation of fibrillated crazes within these particles [Fig. 2(a)].

In contrast to diblock copolymers, where the deformation zones are highly localized,[4,5,14] both PS and the PB lamellae are homogeneously deformed, which demonstrates that the PS lamellae show a large plastic deformation over the entire specimen.

Microvoids are heavily stained by OsO_4 in different regions, as shown in Figure 2(b,c). In addition to the staining effect, OsO_4 has an affinity to be deposited at regions with a larger free volume (microvoids). Dark spots formed by heavy deposi-
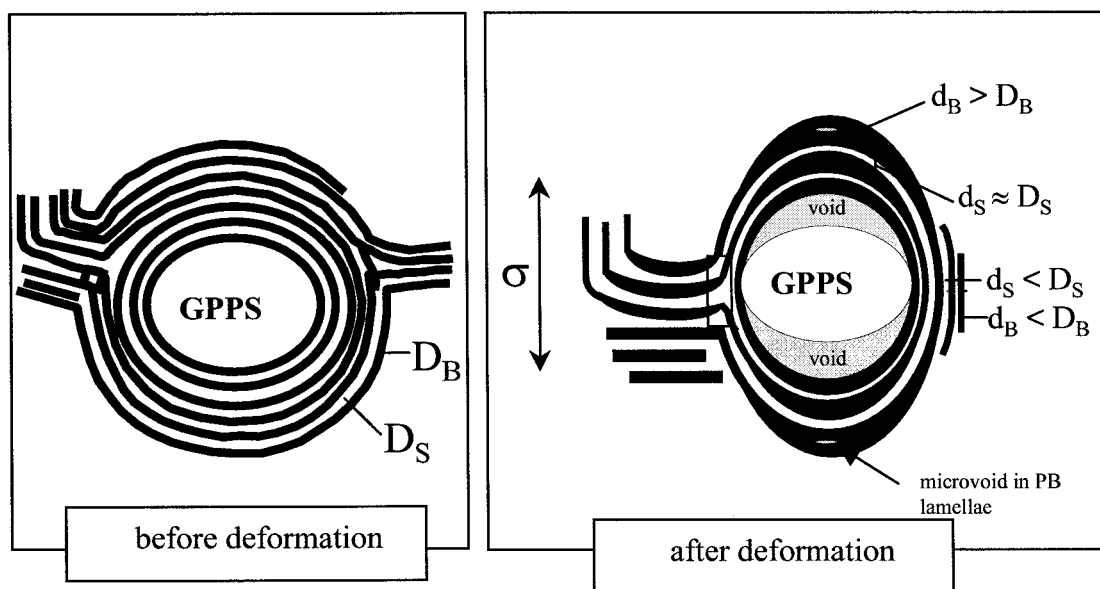
$$D_S, D_B \quad \text{thickness of PS and PB lamellae before deformation}$$
$$d_S, d_B \quad \text{thickness of PS and PB lamellae after deformation}$$

Figure 3 Schematic drawing showing different degrees of lamellae deformation depending on their orientation (parallel, perpendicular, or tilted toward the external stress).

tion of staining agent can be observed in PB lamellae which lie perpendicular to the stress direction. This indicates that the PB lamellae are preferentially deformed followed by void formation, which was also reported by Yamaoka.[27] The deformation behavior observed in sample I is summarized schematically in Figure 3.

Mechanical Properties

In Figure 4 the tensile properties of sample I are compared with that of pure GPPS. The star block copolymer shows a lower modulus, a relatively low yield strength, and a large strain at break (about 240%). At higher strains, the stress shows a strong increase which is well known from other polymers as strain hardening. This leads to a tensile strength of 33 MPa, which is about 40% smaller than that for pure GPPS.

The total amount of PS in sample I (including the GPPS) is about 85%. Compared to HIPS which contains about the same amount of rubber, the toughness of the star block copolymer is much higher. In contrast to rubber-toughened PS possessing an equivalent amount of rubber which shows a tensile strength of about 20–30 MPa and a strain at break of about 20–40%,[2] sample I has a tensile strength of 33 MPa and a strain at break

of 240%. It should be, however, kept in mind that specimens of sample I used for tensile tests were much smaller than standard tensile specimens used for injection-molded samples II and III. Reasons for high toughness of sample I will be discussed in the following sections on the basis of the discussion of micromechanical behavior.

Discussion

Sample I (ST2-S74 containing 17 wt % of GPPS) was prepared by using toluene as solvent. Hence, the lamellar arrangement of PS and PB represents the equilibrium structure of the star block copolymer. It is quite interesting that small PS domains are observed inside the PB lamellae in all samples. This observation is related to the special molecular architecture of the star block copolymer and will be discussed in Part II of this study.

Although sample I principally shows a homogeneous deformation revealed by the large plastic deformation of lamellae, the degree of this deformation is mainly determined by the orientation of lamellae toward tensile direction. Because the lamellae are oriented randomly arising from solvent casting, an anisotropic deformation behavior on the microscopic scale is observed. This type of
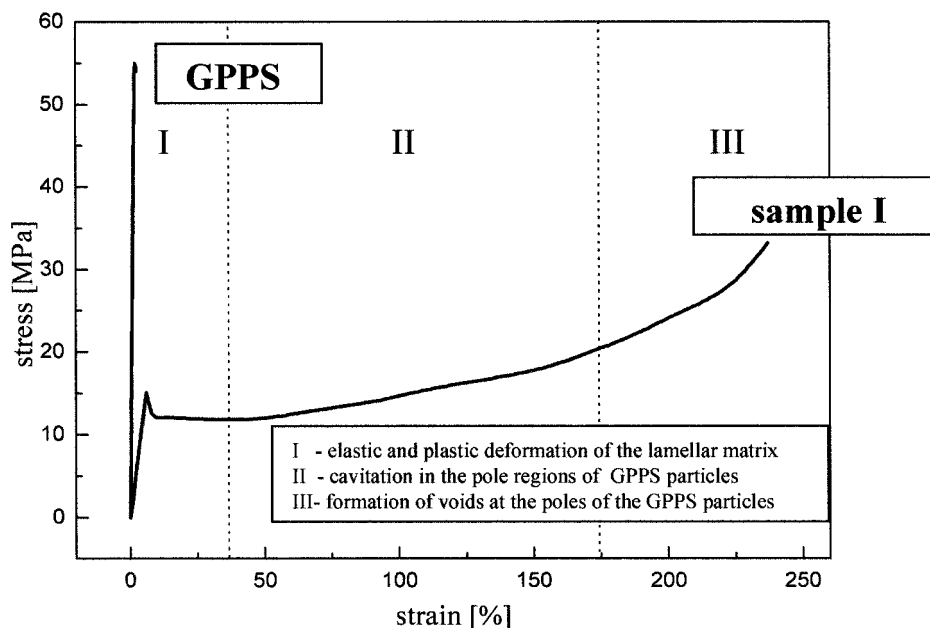
Figure 4 Stress–strain curve of sample I (ST2-S74 with GPPS particles) compared with that of pure GPPS; regions I, II, and III represent different states of deformation in the sample during tensile testing.

anisotropy in deformation behavior resulting from different orientation of lamellae is well known from semicrystalline polymers.[28]

Both PS and PB lamellae situated parallel to the strain direction are largely deformed. Quantitative analysis revealed that thickness of these PS and PB lamellae is reduced to less than 50%. If the lamellae lie normal to the tensile direction, the PB lamellae are preferentially deformed (about 20%) and the PS lamellae remain almost undeformed. These PB lamellae are cavitated because of their low strength, as revealed by the heavily stained spots found in the PB lamellae (see Fig. 2). Cavitation as the dominating deformation mechanism in many rubber-toughened polymers and diblock copolymers has been reported by many authors. Recently, the plastic deformation of the PS matrix initiated by cavitation of PB cylinders in SB diblock copolymer was investigated[14] and accepted as a principal deformation mechanism in diblock copolymers.[5]

In contrast to diblock copolymers, where a local cavitation mechanism can be observed, the investigated star block copolymers show a homogeneous deformation. As shown in Figure 2, a more diffuse cavitation in PB occurs, confirming the homogeneous characteristics of deformation in this sample. In contrast to diblock copolymers, a

growth of crazes via two-step cavitation mechanism is not observed.

Deformation mechanism revealed by TEM investigations can be correlated with results of tensile tests. In the first region (I) of the stress–strain curve in Figure 4, the PS and the PB lamellae show an elastic deformation. At the yield point, the onset of plastic deformation of PS lamellae can be found. In the second region (II), cavitation at the poles of GPPS particles takes place, which is a consequence of disentanglement of PS chains in the GPPS phase and the PS lamellae. Cavitation at the poles of the GPPS particles acts as precursor for further plastic deformation of lamellar matrix which surrounds GPPS particles and voids. Further, growth of these microvoids occurs via large plastic deformation of PS and PB lamellae, which surround the GPPS particles and microvoids [Fig. 2(b)]. Quantitative analysis of the thickness of lamellae and the long period determined from the TEM micrographs is shown in Table II. It is seen in Table II that these values are significantly reduced to about half because of deformation of the samples.

At large deformations (more than 200%, region III in Fig. 4), a macroscopic stress whitening occurs in the tensile specimens. This arises from the growth of microvoids around the GPPS particles. This process is accompanied by a formation of

Table II Thickness of PS Lamellae (D_{PS}) and Long Period (*L*) in the Samples Before and After Deformation

	Before Deformation			After Deformation			
Sample	D_{PS} (nm)[a]	L (nm)[b]	L_{mean} (nm)[c]	D_{PS} (nm)[a]	L (nm)[b]	L_{mean} (nm)[c]	D_{PS} in def. zone (nm)
I	10–20	35–43	—	5–9	18–35	—	—
IIa	10–20	25–40	40	7–12	15–25	21	—
IIb	10–32	34–54	42	8–22	12–26	18	—
III	10–20	35–40	32	10–20	30–35	31	7–12

[a]Determined by analysis of TEM images by special image processing program.
[b]Determined by FTA of TEM images.
[c]Mean lamellar long period.

additional cavities at the poles of smaller GPPS particles and in the PB lamellae (see Figs. 2 and 3). As already mentioned, the deposition of the staining agent (i.e., OsO_4) in the PB lamellae situated perpendicular to the strain direction indicates that the PB lamellae are preferentially deformed. The initial deformation of PB lamellae occurs in an adjacent position at the poles of the GPPS particles and in lamellae perpendicularly oriented to the external stress direction. The ultimate fracture of the specimen occurs via growth of microvoids, resulting in cracks and critical crack propagation.

Homogeneous plastic deformation of PS lamellae is the most striking effect observed in this material. As a result of plastic deformation, the thickness of PS lamellae decreases from about 10–20 nm to 5–9 nm (i.e., a thickness reduction of about 50%, see Table II). The same order of decrease in thickness of lamellae might be expected for the width of the lamellae (i.e., in the direction normal to the micrographs). From this, an elongation of about $\lambda \approx 4$ can be estimated, which is of about the same order as the strain at break of bulk specimen. Moreover, this elongation is in same order as the maximum elongation of craze fibrils in PS.[2,29] Elongation of craze fibrils is limited by entanglements. The maximum extension, λ_{max}, of craze fibrils is correlated to the maximum deformation ratio of the entanglement network given by $\lambda_{max} = l_e/d \approx 4$, where l_e is the contour length between the adjacent entanglement points and d is the root-mean-square end-to-end distance of a chain corresponding to entanglement molecular weight.[2,29]

Homogeneous deformation of craze fibrils in PS appears if the thickness of the fibrils lie in the range of about 5–20 nm.[2] In star block copolymers, the homogeneous deformation of PS lamellae is similar to homogeneous craze fibril deformation in PS. Hence, this deformation mechanism in star block copolymers can be called thin-layer yielding. In contrast to the cavitation mechanism which is usually observed in block copolymers,[5,14] a homogeneous deformation of PS lamellae as well as of adjacent PB lamellae occurs and local deformation zones or crazes are not observed in this star block copolymer. The thickness of the adjacent PB lamellae in the lamellar block copolymer should be taken into account to consider the yielding mechanism of thin PS lamellae. This effect will be described in more detail while discussing the results of sample III.

To summarize the above discussion, a new toughening mechanism called thin-layer yielding is proposed. The principle of this thin-layer yielding mechanism is schematically represented in Figure 5.

A brittle material with a layer thickness D acts brittle (characterized by low strain at break, ϵ_B) as far as the value D is above a critical thickness (about 20 nm). Below this thickness, a strong transition to a very ductile fracture mode (large elongation to break, ϵ_B) occurs. Results observed in lamellae-forming star block copolymers indicate that this effect can be used as an alternative toughening mechanism in block copolymers.

The reported deformation mechanism of star block copolymer is the result of the modified molecular architecture compared to the common diblock copolymers. First, the larger number of arms in star block copolymers enable a better molecular coupling even at low molecular weights. At low molecular weights, the properties of diblock copolymers show a molecular weight dependence. This means that in diblock copoly-
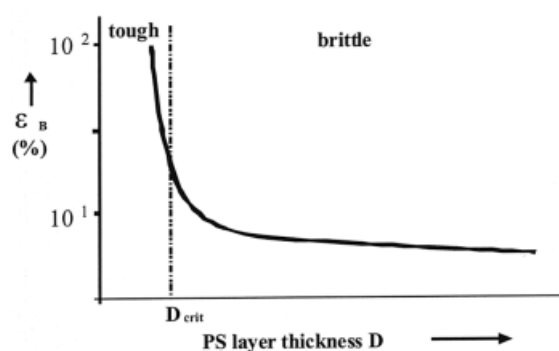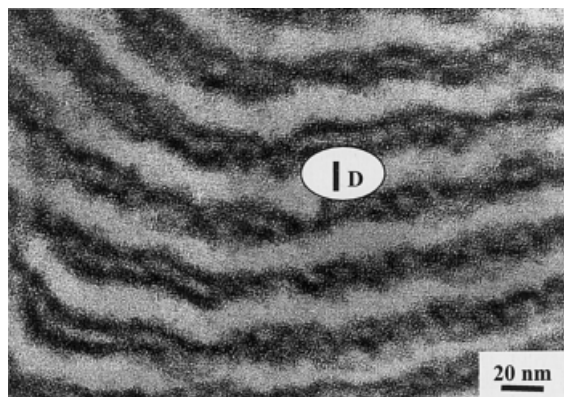
Figure 5   Schematic drawing of principle of thin-layer yielding mechanism. D, $D_{Crit,}$ and ϵ are thickness of PS lamellae, their thickness, and maximum elongation, respectively.

mers with the same lamellae thickness a thin-layer yielding mechanism cannot be observed because of the low molecular weight of the corresponding blocks, which are unable to form entanglements. Thus, PS-*b*-PB diblock copolymers with total molecular weights of about 100,000 g/mol appear to be quite brittle. However, for diblock copolymers with higher molecular weights, the long period increases and therefore the thickness of lamellae do not fulfill the conditions proposed in Figure 5.

Second, the presence of chemically coupled chains in block copolymers is responsible for a more effective stress transfer between the adjacent lamellae.

Third, the presence of a broadened interface width clearly causes an additional improvement of mechanical properties, as discussed in Part II of this study. This is, of course, again correlated to deformation behavior, as discussed in detail in ref.[5]

Samples with Lamellar Structure, Without GPPS Particles, and with Neck Formation During Tensile Testing (IIa, ST2-S74 with 14 wt % of GPPS prepared by injection molding, and IIb, ST2-S74 pure prepared by injection molding)

Morphology

Both samples possess alternating PS and PB lamellae [Fig. 6(a,b)], very similar to that of sample I. These samples, however, exhibit no GPPS particles. The thickness D and long period L of PS lamellae are summarized in Table II.

A typical morphology of sample IIa is given in Figure 6(a). The most striking difference between sample I and IIa is the orientation of the lamellar morphology. This difference arises from the fact that sample IIa was prepared by injection molding. Preferential orientation of lamellae in flow direction results from the shear forces operating parallel to the flow direction. Sample IIa shows no indication of a macrophase separation, although it contains 14% GPPS. GPPS has a large molecular weight distribution with a the low molecular weight fraction, which is solubilized in the corresponding block of the star block copolymer. Moreover, a part of GPPS with molecular weight higher than that of the corresponding block of the star block copolymer might be mixed with the corresponding lamellae of the block copolymer because of large shear stress in the injection-molding process. It is known from polymer blends and block copolymers that shear stress can lead to a significant change of morphology. Therefore, the difference in morphology between solvent-cast specimens and injection-molded samples results from the influence of shear stresses during injection molding. In contrast, solvent-cast sample I shows an equilibrium morphology without a preferential orientation of lamellae.

Sample IIb has a similar morphology as sample IIa where the lamellae are aligned in a parallel direction to the flow direction with small PS domains in the PB lamellae. Sample IIb is a star block copolymer without an additional homopolymer and, therefore, macrophase-separated PS particles cannot be found in this material.

It should be mentioned, however, that the PS lamellae in the sample IIa [Fig. 6(a)] appear more continuous, whereas lamellae in sample IIb [Fig. 6(b)] look more or less wormlike in structure. The reason for this difference might be the additional amount of homopolymer in sample IIa.
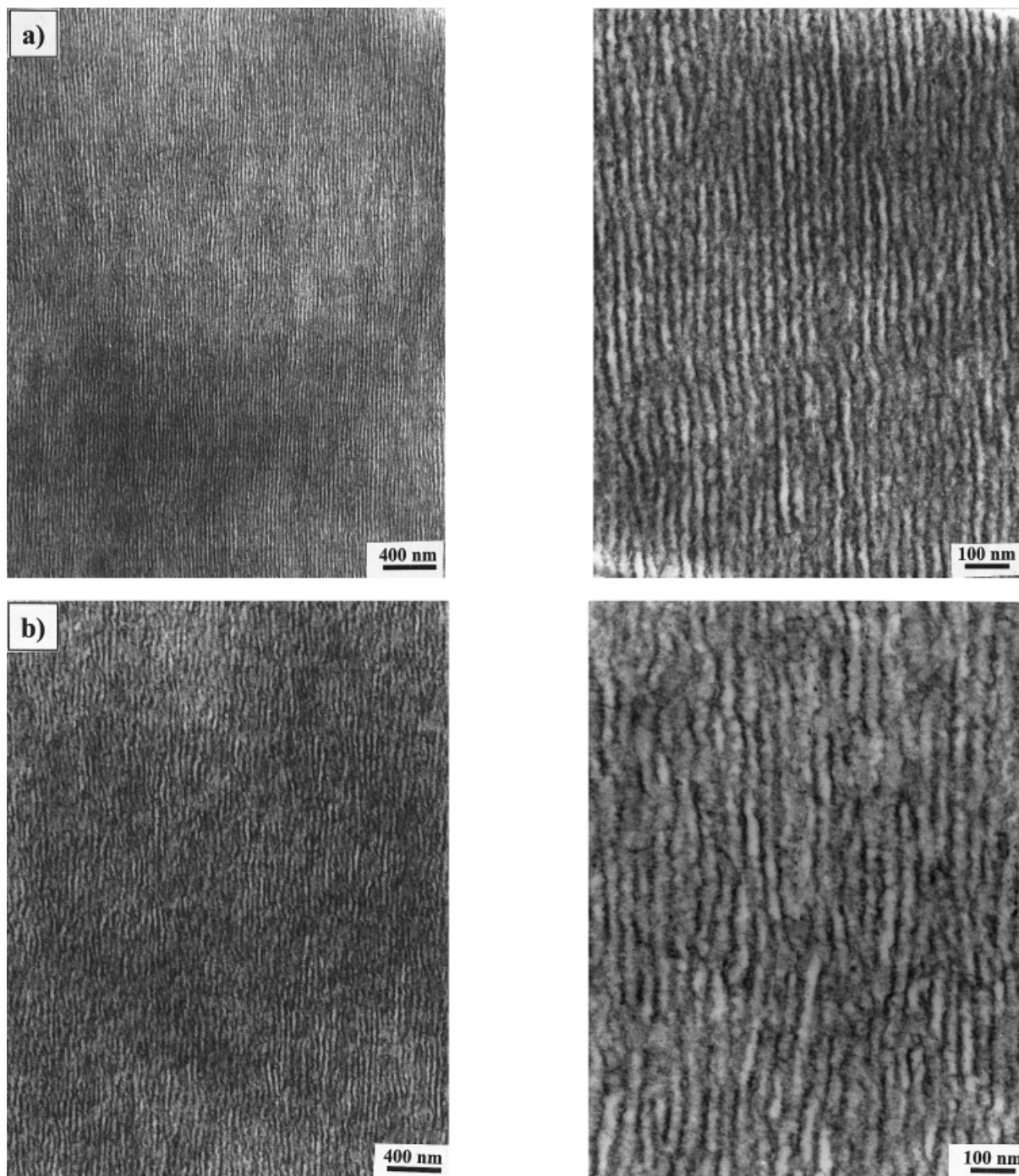
Figure 6 Lower (left) and higher (right) magnifications of TEM micrographs of injection-molded specimens of sample IIa (a, top) and Sample IIb (b, bottom), injection-molding direction vertical.

Micromechanical Deformation Mechanism

The micromechanical mechanism observed in samples IIa and IIb is the thin-layer yielding mechanism already observed for sample I. The absence of GPPS particles and the highly oriented lamellar morphology in these samples result in homogeneous deformation structures, as shown in Figure 7.

Figure 7(a) shows the deformation structure after tensile testing of sample IIa. The lamellae are oriented parallel to the direction of external
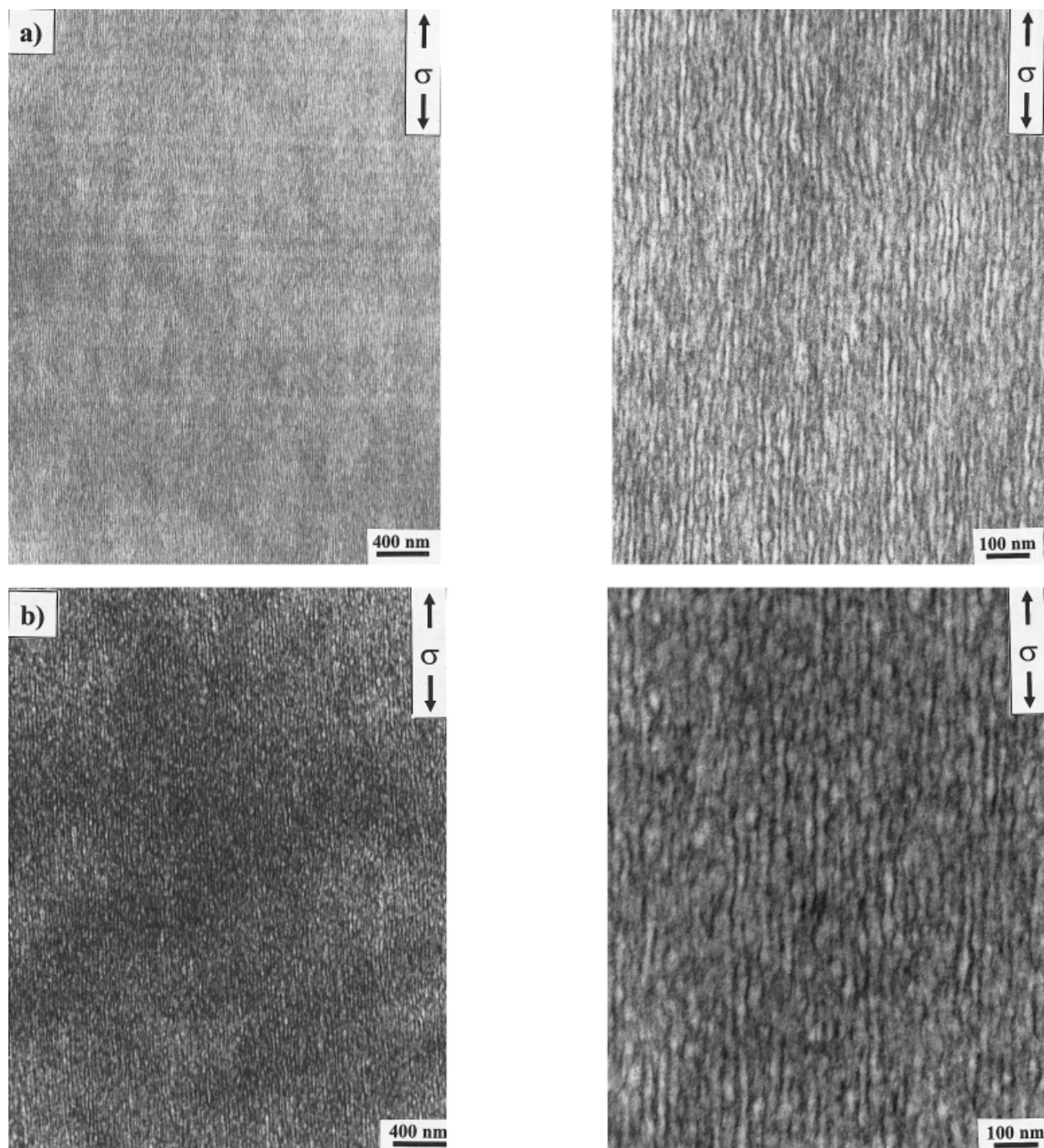
Figure 7   Lower (left) and higher (right) magnifications of TEM micrographs showing the morphological changes in deformed sample IIa (a, top) and sample IIb (b, bottom) after tensile tests. Tensile direction vertical (i.e., parallel to lamellae orientation).

stress and both the PS and the PB lamellae are deformed together. There are no local deformation zones, indicating a homogeneous deformation of both types of lamellae in the direction of external stress. There is also no diffuse cavitation of PB lamellae as it was observed for sample I, be-

cause there are no PB lamellae oriented perpendicular to external stress.

Figure 7(b) shows the deformation structure of sample IIb. Both PS and PB lamellae are highly deformed to the direction of applied stress, which is clearly shown by the decrease of the long period
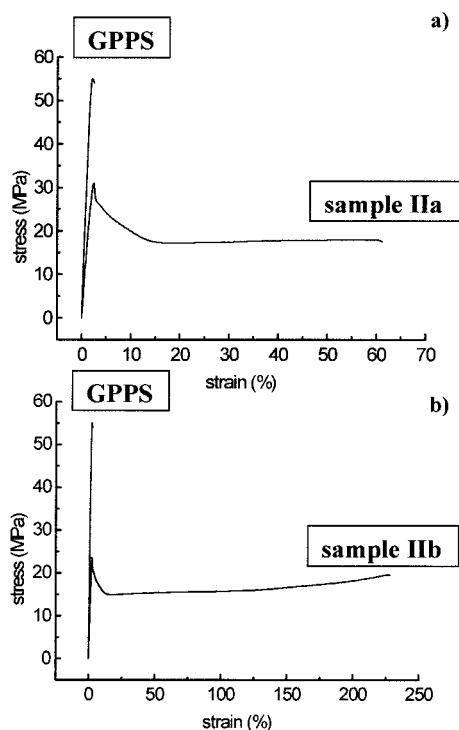
Figure 8 Stress–strain curves of sample IIa (a) and sample IIb (b) compared to GPPS.

and thickness of the PS lamellae in Table II. PS lamellae are fragmented into short pieces of lamellae. Formation of microvoids in the PB phase is not observed in this sample also.

The difference in orientation of lamellae is the reason for the observed change of deformation structure. The existence of a preferential orientation of the lamellae in the direction of external stress enables a large deformation of both lamellae. In the case of randomly oriented lamellae (sample I), a cavitation of PB lamellae can occur in regions where the lamellae are perpendicularly oriented to the external stress. The difference between deformation structure of sample IIa and IIb might be attributed to the additional PS con-

tent in sample IIa, which increases the strength of PS lamellae and reduces the ultimate elongation at break. The large elongation of sample IIb yields to the fragmentation of PS lamellae before macroscopic failure of the specimen.

Mechanical Properties

In Figure 8, the tensile properties of samples IIa and IIb are compared with pure GPPS (strain rate = 50 mm/min, room temperature). Tensile specimens are deformed via neck formation and subsequent extension of this neck. Both samples have a higher yield stress (28 and 24 MPa, respectively) than the solution-cast sample I (about 16 MPa; see Table III). In contrast to sample IIb which shows strain hardening (strain at break of 257%), sample IIa shows a strain softening after the yield point accompanied by premature failure at a strain of only about 50%.

To investigate the dependence of mechanical properties on strain rate and temperature, injection-molded specimens of sample IIa were investigated at different strain rates (from 15 up to 200 mm/min) and temperatures (room temperature, 0°C, and −30°C). The results are summarized in Table IV.

It is shown in Table IV that the tensile properties strongly change with temperature, reflecting a change in deformation behavior in the samples. The strain at break decreases with increasing strain rate and decreasing temperature. At room temperature, samples show a macroscopic neck formation and subsequent elongation. A transition from macroscopic neck formation with elongation to neck formation without neck elongation takes place with increasing strain rate or decreasing temperature. An increase of strain rate has the same result as a decrease of temperature, as it was also observed for other polymers.

Discussion

The deformation mechanism of lamellae observed in samples IIa and IIb is principally the same as

Table III   Mechanical Properties of Star Block Copolymers Determined by Uniaxial Tensile Tests, 50 mm/min at room temperature

Sample	Young's Modulus (MPa)	Yield Strength (MPa)	Tensile Strength (MPa)	Strain at Break (%)	Remarks
I	—	16	33	240	Solvent cast film
IIa	1520	28	28	50	Injection moulded
IIb	1205	24	28	257	Injection moulded
IIb	—	22	26	320	Solvent cast film
III	1760	34	34	10	Injection moulded

Table IV   Mechanical Properties of Injection-Molded Sample IIa (ST2-S74 with 14 wt % GPPS, injection-molded) Observed at Different Strain Rates and Temperatures

Temperature (°C)	Crosshead Speed (mm/min)	Tensile Strength (MPa)	Strain at Break (%)
Room temp.	15	25	215
	30	26	148
	50	28	50
	100	29	25
	200	30	20
0	15	36	40
	50	38	15
−30	15	46	20

observed in sample I (thin-layer yielding mechanism). A homogeneous deformation of PS and PB lamellae occurs, resulting in a decrease in lamellae thickness D and long period L (Table II). The drastic reduction of these values in sample IIb is in accordance with observed strain at break of 257%. This large elongation at break is associated with a fragmentation process of PS lamellae and a more pronounced tendency of strain hardening.

Premature failure of sample IIa can be understood in the context of discussed dependence of thin-layer yielding mechanism on thickness of lamellae (see Fig. 5). If the thickness of PS lamellae are increased by addition of PS, a critical value of PS lamellae may be achieved where a ductile to brittle transition becomes more probable.

A comparison of sample I (ST2-S74 containing GPPS particles, solution cast film) with sample II is difficult because injection-molded tensile specimens have a larger size than solution cast films. Therefore, sample IIb was also prepared as solution-cast films. The lower yield stress of sample I compared to that of sample IIb can be explained by the influence of PS particles on deformation behavior. In the case of sample I, microvoid formation at the poles of GPPS particles results in stress concentrations in the adjacent matrix. Therefore, the local yield stress of PS lamellae is reached at a lower external stress.

Star Block Copolymer with Lamellar Structure, Without GPPS Particles, and Without Necking During Deformation (Sample III ST2-S80 Containing 17 wt % of GPPS, injection molded)

Morphology

Sample III reveals a morphology of alternating PS and PB lamellae, as shown in Figure 9. The lamellae are oriented because of the injection-molding process. Thickness and long period of PS lamellae observed in this sample are in the range of 10–20 nm and 35–40 nm, respectively (see Table II). The thickness of PB lamellae is smaller than that for other samples, arising from the smaller volume fraction of PB in this sample. It is seen in Figure 9 that the interface between both phases is not sharp. This is due to the higher miscibility of both blocks arising from the tapered transition in this type of star block copolymer. A broadened interface can also be expected for other samples investigated in this study, which will be discussed in detail in Part II.

Micromechanical Deformation Mechanism

Figure 10 shows the deformation structures observed in sample III. In contrast to the homogeneous thin-layer yielding mechanism observed in samples I and II, highly localized deformation bands are observed. These bands often propagate perpendicularly to the direction of external stress. Some of these bands are tilted at about 45° toward the stress direction. These deformation zones resemble crazes with respect to their location (the bands propagate perpendicularly to the tensile direction). Inside the deformation bands, the PS and PB lamellae are highly deformed with a microstructure tilted at about 50° toward the direction of external stress. No significant changes in thickness and long period of lamellae are observed outside the deformation bands (see Table II).

Mechanical Properties

In Figure 11, stress–strain curves of sample III and pure PS are compared. Sample III has the
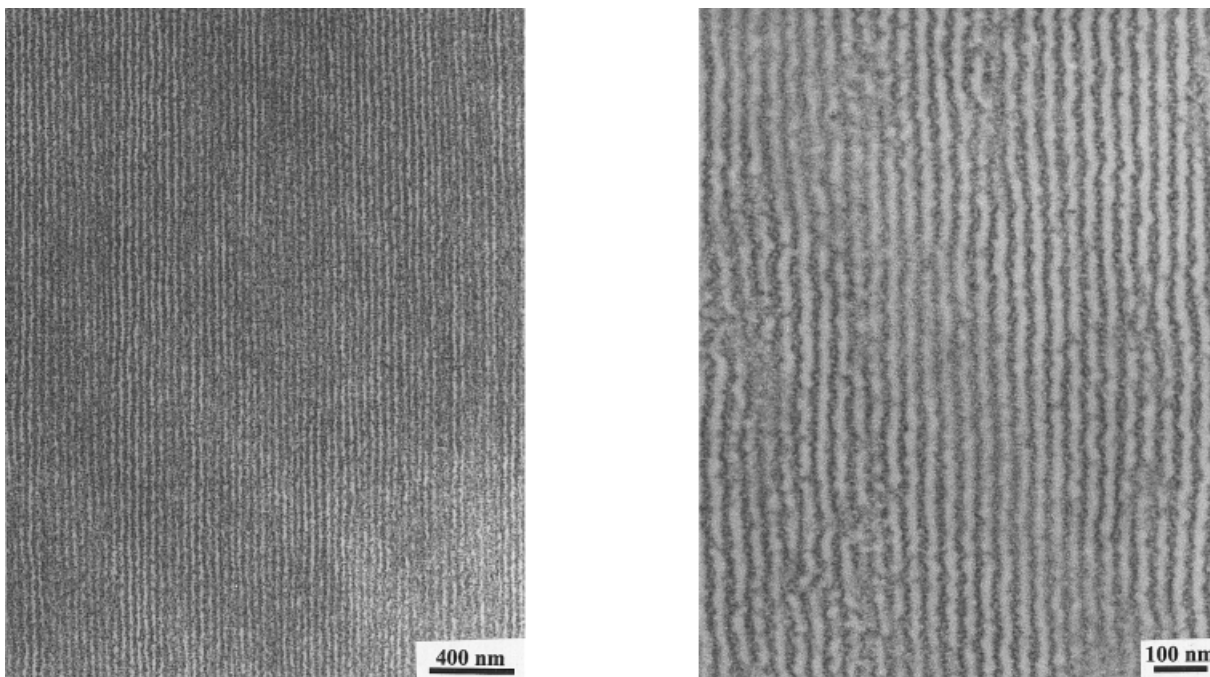
Figure 9 Lower and higher magnifications of TEM micrographs showing morphology of injection-molded sample III (ST2-S80 without GPPS particles); injection direction vertical.

highest yield strength but the lowest strain at break of all the investigated star block copolymers (Table III). This indicates a change of deformation mechanism in agreement with our TEM observations.

The reduction of volume fraction of PB is associated with a significant decrease of strain at break, indicating that a minimum volume fraction of PB is necessary for tough behavior.

Discussions

Sample III is deformed via formation of local deformation bands, which show the characteristics of both crazes (with respect to their orientation to the external stress direction) and shear bands (with respect to tilt angle of microstructure inside the deformation bands toward the external stress direction). These local deformation bands are very different from conventional crazes or shear bands observed in homopolymers similar to PS and rubber-toughened thermoplastics.[2] Unlike crazes, there is no evidence of voiding, and unlike shear bands, the deformation bands usually are not tilted at 45° toward the direction of stress. The lamellae inside these deformation bands are highly deformed. The thickness of the PS lamellae inside the bands is reduced to about 50% (see Table II). However, the strain at break of sample

III is about 10%, which is caused by the deformation of lamellae inside these deformation bands alone. The exact mechanism of growth of these deformation bands is not fully understood and requires further investigation. We believe that the molecular architecture of the star block copolymers has a large influence on deformation of lamellae.

The highly deformed PS lamellae inside the deformation bands look like they were relaxed after the external stress is released. This is indicated by the wavy pattern of the lamellae which might be a result of a partial relaxation to their original state. This relaxation is connected with the tilt angle of lamellae inside the deformation bands toward a certain angle (about 50° in the present case).

Significant change in mechanical properties (especially the decrease in strain at break) of sample III is related to the change of deformation mechanism from homogeneous deformation of lamellae to formation of local deformation zones. A homogeneous deformation of PS lamellae is possibly hindered by the insufficient size of the PB layers between the PB lamellae. The deformation only occurs in the deformation zones, which results in a significant decrease in strain at break of sample III.
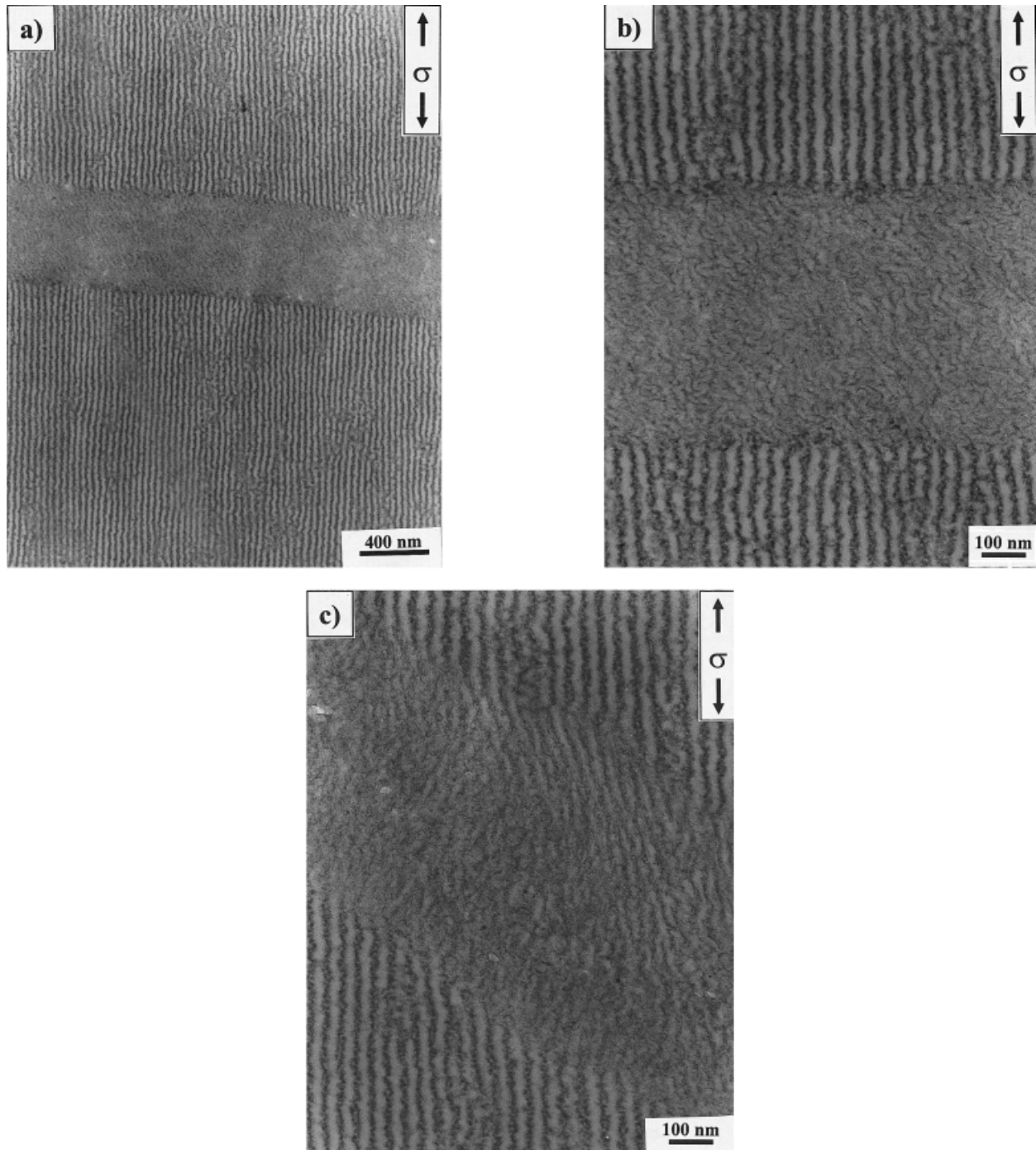
Figure 10 TEM micrographs showing deformation structures in sample III (ST2-S80 without GPPS particles); tensile direction vertical (i.e., parallel to the lamellar orientation).

CONCLUSION

In styrene/butadiene star block copolymers with lamellar morphology, a new deformation mechanism was found—the homogeneous yielding of PS lamellae together with adjacent PB lamellae. The PS lamellae are homogeneously deformed up to 300% without cavitation or microvoid formation. This is an effect of a thin-layer yielding mechanism, appearing in thin PS lamellae with a thick-
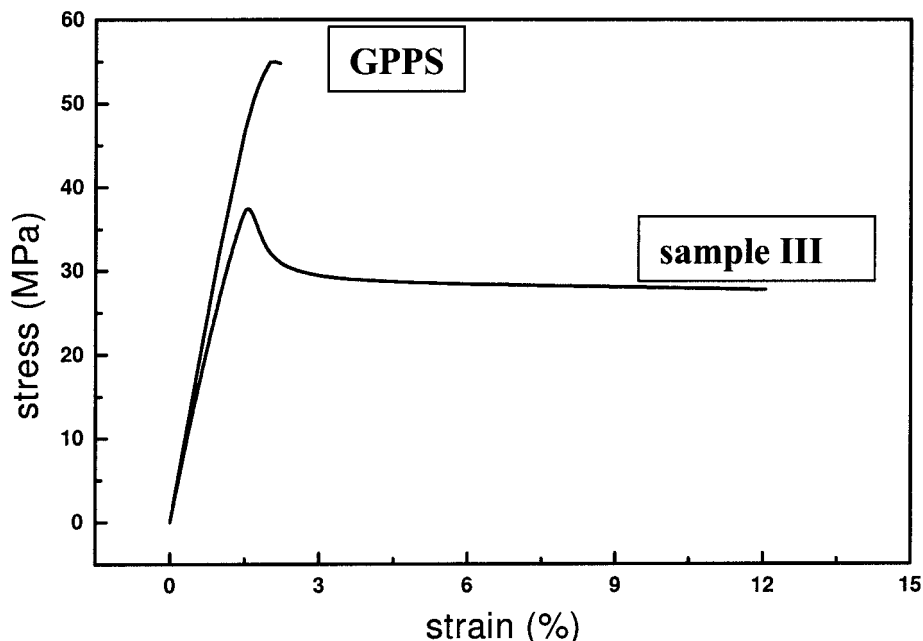
Figure 11 Stress–strain curves of injection-molded specimens of sample III compared to pure GPPS.

ness smaller than the critical thickness. The critical thickness D_{crit} can be compared with the maximum thickness of the craze fibrils in PS (i.e., in the range of 20 nm). The difference between both mechanisms can be seen in the fact that craze fibrils in PS are stretched between microvoids, whereas the PS lamellae are deformed together with the adjacent PB lamellae. Therefore, the PB lamellae may have a function analogous to that of adjacent microvoids and do not hinder the deformation of PS lamellae. It can be assumed that the PB lamellae possess only a small load-bearing capacity. The load is carried mainly by the PS lamellae with an effect of stress concentration. At a PB content of about 30%, stress concentration in the PS lamellae can be expected to be about 1.4 times higher than the externally applied stress. By using this value and the yield stress determined by tensile testing of about 24 MPa (Fig. 8), the internal yield stress of the PS lamellae can be estimated to $\sigma_y^{lam} \approx 34$ MPa. This is significantly lower than the yield stress of 55 MPa for bulk PS (the crazing stress in PS is on the order of 55 MPa[21,30]). Therefore, the schematic drawing in Figure 5 can be redrawn as shown in Figure 12.

Below the critical thickness of PS lamellae, the yield stress of PS lamellae σ_y^{lam} is sufficiently low to induce a large plastic flow of PS lamellae leading to the ductile behavior of the star block co-

polymer. If the thickness of PS lamellae exceeds the critical value of about 20 nm, a strong increase in yield stress of PS lamellae occurs too. Hence, the yield stress of thick PS lamellae reaches the crazing stress of PS. Deformation leads to the formation of crazelike deformation zones and the polymer becomes brittle.

It may be anticipated that the critical thickness of glassy layer further depends on the deformation speed and temperature. With increasing deformation rate and decreasing temperature,
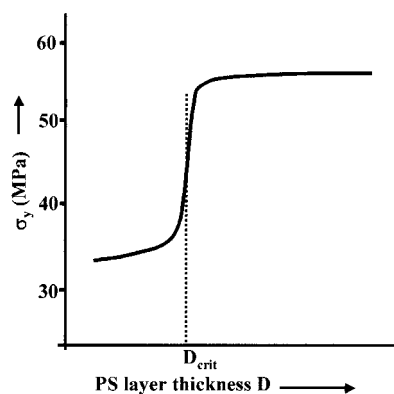

Figure 12 Mechanism of thin-layer yielding: yield stress of PS lamellae as a function of lamellae thickness.

the molecular relaxation processes are hindered, which may probably shift the critical thickness toward the lower value. Micromechanical studies with variation of strain rate and temperature are under way to clarify the deformation speed and temperature dependence of thin-layer yielding mechanism.

It should be kept in mind that besides the influence of thickness of lamellae, the molecular architecture and the interface between both components play an important role in the mechanical properties and deformation mechanisms. Both aspects (molecular architecture and nature of the interface) will be discussed in Part II of this study.

REFERENCES

1. Michler, G. H. in Polymeric Materials Encyclopedia; Salamone, J. S., Ed.; CRC Press: London, 1996.
2. Michler, G. H. Kunststoff-Mikromechanik, Morphologie, Deformations, und Bruchmechanismen; Carl Hanser: München, 1992.
3. Starke, U. J.; Godehardt, R.; Michler, G. H.; Bucknall, C. B.; J Mater Sci 1997, 32, 1855.
4. Weidisch, R.; Michler, G. H.; Arnold, M.; Hofmann, S.; Stamm, M.; Jerome, R. Macromolecules 1997, 30, 8078.
5. Weidisch, R.; Enβlen, M.; Michler, G. H.; Fischer, H. Macromolecules 1999, 32, 5375.
6. Breiner, U.; Krappe, U.; Jakob, T.; Abetz, V.; Stadler, R. Polym Bull 1998, 40, 219.
7. Breiner, U.; Krappe, U.; Thomas, E. L.; Stadler, R. Macromolecules 1998, 31, 315.
8. Hamley, I. The Physics of Block Copolymers; Oxford Science Publications: Oxford, 1998.
9. Abetz, V.; Goldacker, T. Macromol Rapid Commun 2000, 21, 16.
10. Mogi, Y.; Nomura, M.; Kotsuji, H.; Matsuhita, Y.; Noda, I. Macromolecules 1994, 27, 6755.
11. Drolet, F.; Fredrickson, G. H. Phys Rev Lett 1999, 83, 4317.
12. Bohbot-Raviv, Y.; Wang, Z.-G. Phys Rev Lett 2000, 85, 3428.
13. Argon, A. S.; Cohen, R. E. in Advances in Polymer Science 91/92, Crazing in Polymers—Vol. II; Kausch, H. H., Ed.; Springer-Verlag: Berlin, Heidelberg, 1989; p 301.
14. Schwier, C. E.; Argon, A. S.; Cohen, R. E. Polymer 1985, 26, 1985.
15. Asthana, S.; Kennedy, J. P. J Polym. Sci, Part A: Polym Chem 1999, 37, 2235.
16. Shim, J. S.; Kennedy, J. P. J Polym Sci, Part A: Polym Chem 1998, 37, 815.
17. Quirk, R. P.; Morton, M. in Thermoplastic Elastomers, 2nd ed.; Holden, G., Legge, N. R., Quirk, R. P.; Schroeder, H. E., Eds.; Hanser Publishers: Munich, 1998; Chapter 4.
18. Sameth, J.; Spontak, R. J.; Smith, S. D.; Ashraf, A. Mortensen, K. J Phys 1996, 3, 59.
19. Asai, S. Polym Prepr 1996, 37, 706.
20. Moctezuma, S. A.; Martinetz, E. N. in ACS Symposium Series: Applications of Anionic Polymerisation Research; 1998, 696, 129.
21. Knoll, K.; Nieβner, N. Macromol Symp 1998, 132, 231.
22. Winey, K. I.; Thomas, E. L.; Fetters, L. J. Macromolecules 1994, 25, 422.
23. Koizumi, S.; Hasegawa, H.; Hashimoto, T. Macromolecules 1994, 27, 7893.
24. Hasegawa, H.; Hashimoto, T. in Comprehensive Polymer Science, Suppl. 2; Aggarwal, S. L., Russo, S., Eds.; Pergamon: London, 1996.
25. Kim, G.-M.; Michler, G. H. Polymer 1998, 39, 5689.
26. Kim, G.-M.; Michler, G. H. Polym Adv Technol 1998, 9, 709.
27. Yamaoka, I.; Kimura, M. Polymer 1993, 34, 4399.
28. Li, J. X.; Cheung, W. L.; Chan, C. M. Polymer 1999, 40, 2089.
29. Kramer, E. J. J Polym Eng Sci 1984, 24, 761.
30. Young, R. J. Introduction to Polymer Science; Chapman and Hall: London, 1989.